



Abrasive water jet machining of glass fibre reinforced polymer composite: experimental investigation, modelling and optimization

Anil Kumar Dahiya^{1,2} · Basanta Kumar Bhuyan¹ · Shailendra Kumar³

Received: 24 September 2022 / Accepted: 20 March 2023 / Published online: 21 April 2023
© The Author(s), under exclusive licence to Springer-Verlag France SAS, part of Springer Nature 2023

Abstract

This paper describes an experimental investigation, modelling and optimization during abrasive water jet machining (AWJM) of glass fibre reinforced polymer composite. Four process parameters namely water pressure, stand-off distance, traverse rate and abrasive mass flow rate are considered to study their influence on maximum delamination length (Max. DLL), surface roughness (R_a) and kerf taper (K_t). The second-order regression models are developed for the maximum delamination length, surface roughness and kerf taper in AWJM of glass fibre reinforced polymer composite using response surface methodology based central composite design approach. From the regression models, it is revealed that delamination decreases with an increase in abrasive mass flow rate, with a decrease in traverse rate. Surface roughness decreases with increase in water pressure and decrease in traverse rate. Kerf taper decreases with increase in water pressure; and decrease in traverse rate and stand-off distance. Further, response surface methodology based desirability function is performed to minimize the Max. DLL, R_a and K_t and the desirability values were found for $R_a = 0.936$, $K_t = 0.942$ and Max. DLL = 1 with a combined desirability rating of 0.959 which was reasonably good and acceptable. From the confirmation test of multi-response optimization, it was obvious that the percentage error at optimum level of process parameters for R_a , K_t , and Max. DLL were less than 6.312%, 7.229%, and 4.318%, respectively.

Keywords Glass fibre reinforced polymer composite · AWJM · Delamination · Kerf taper · Surface roughness · Regression model · Multi-response optimization

1 Introduction

Glass fibre reinforced polymer (GFRP) composites have applications in various sectors like aerospace, sports, electronics, nuclear energy, transportation, and other similar industries [1]. Machining of composites using traditional machines is extremely complex and expensive because of their exceptional properties like anisotropy and non-homogeneity. In manufacturing industries, abrasive water jet machining (AWJM) has proven to be a cost-effective and efficient metal removal process of composites, in which a high-speed jet of abrasive and water strikes on workpiece

surface to erode material as shown in Fig. 1. High cutting speed, ability to cut in multi-directions, lesser setup time, intricate shapes cutting ability, minimal heat build-up, low deformation stresses, high efficiency, no fumes generation during cutting etc. are the main advantages of AWJM process [2–4]. Drilling, milling, cleaning, hybrid machining, and other machining operations can also be performed reliably and economically and the intricate shapes can be machined with enhanced surface finish [5, 6]. The factors which influence AWJM of composites are categorized based on various process parameters like mixing, cutting, abrasive, and hydraulic [7]. Water pressure (WP), abrasive mass flow rate (AMFR), traverse rate (TR), and standoff distance (SOD) are major process parameters of AWJM.

The main challenges in AWJM of composites are to minimize delamination length (Max. DLL), kerf taper (K_t) and surface roughness (R_a). Delamination is split-up of two adjacent layers of plies in composite laminates as shown in Fig. 2a. During AWJM, the separation of adjacent plies is due to the water wedge action in the composites. It is the

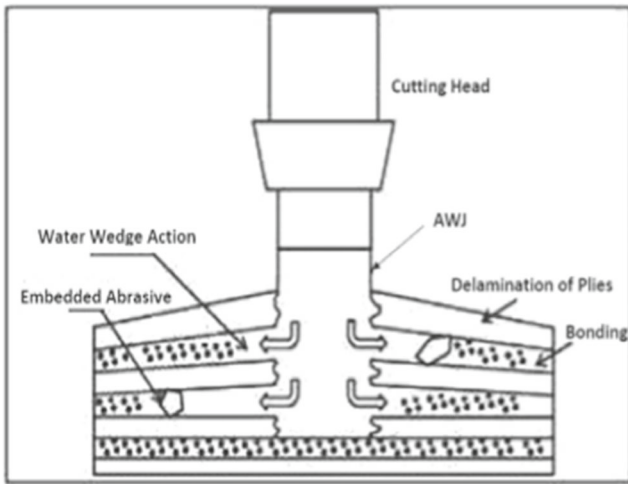
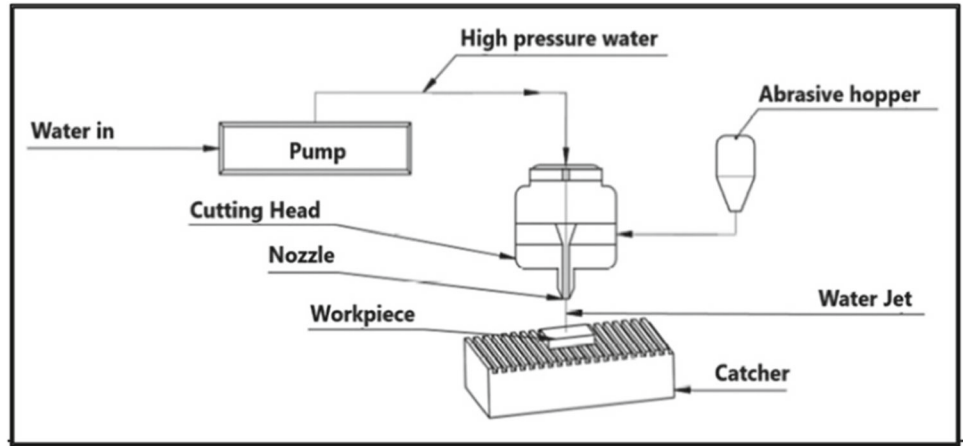
✉ Anil Kumar Dahiya
anildahiya21@gmail.com

¹ Department of ME-FET, MRIIRS, Faridabad, India

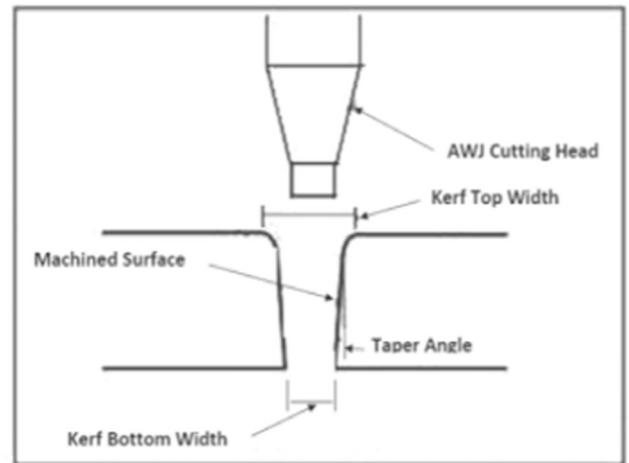
² Department of MAE, Maharaja Agrasen Institute of Technology, Delhi, India

³ Department of ME, SVNIT, Surat, India

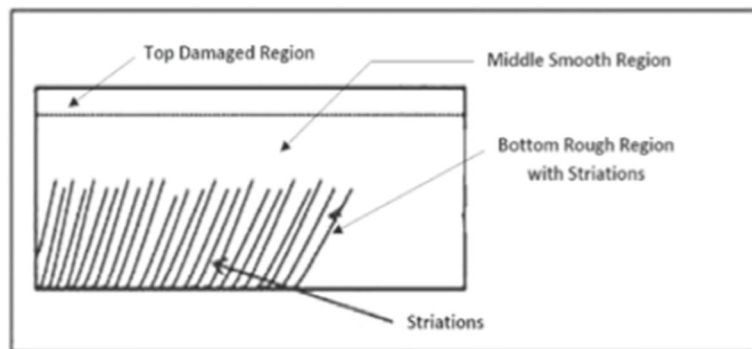
Fig. 1 AWJM process



(a)



(b)



(c)

Fig. 2 a Mechanism delamination and abrasive embedment, b kerf geometry and c machined surface regions

most frequent and dangerous flaw in the machining of GFRP laminate composites. When a jet strikes on a workpiece, it deflects, causing a lateral flow of jet to enter the fragile contact between the composite plies. At these plies, it induces fracture propagation. Delamination occurs when the composite material is subjected to forces that are larger than those required to form the fracture points.

A small rounded corner due to AWJ impingement is produced at the top edge of through cut in machined specimen because of plastic deformation of material. In AWJM, a wider kerf is generated at top as compared to bottom because when the jet penetrates deeper into the specimen, kinetic energy of jet is reduced, resulting in formation of kerf taper. Hence the tapered machined surface is generated as shown in Fig. 2b. Surface produced during AWJM has three different zones namely top damaged zone at the entrance of jet, smooth middle zone and rough bottom zone with striations as highlighted in Fig. 2c. The area of these zones varies with process parameters.

Few attempts have been made to investigate the delamination and kerf geometry mechanism of composites during AWJM. Lemma et al. [8] investigated and compared the normal and oscillation techniques for GFRP composites with AWJ cutting. They found that surface quality improves at high oscillation frequencies. Azmir and Ahsan [9] studied the impact of various parameters on R_a of E-glass fibre composite during AWJM. They reported that abrasive particle hardness, WP, and SOD are substantial parameters for R_a . Shanmugam et al. [10] investigated delamination which occurs due to shock wave generation by jet pressure, water wedging, and abrasive particle embedment in graphite-epoxy composite during AWJM. The impact of various input factors on the kerf width of granite was experimentally investigated during AWJM. For kerf width minimization, low SOD and high TR are recommended. Other parameters for minimum kerf width such as water absorption, weight, microhardness, and mean grain size of granite are less significant [11]. Alberdi et al. [12] investigated the impact of input factors like TR, AMFR, and WP on CFRP/Ti6Al4V stacks during the drilling operation for K_t and R_a with AWJ. They observed that WP, configuration of stack, and TR are the main substantial factors for K_t . K_t and R_a are minimum when Ti6Al4V is used on the upper part of stack. Dhanawade et al. [13] investigated the impact of parameters of AWJ machining on carbon epoxy composite. They reported that K_t and R_a decrease with an increase in WP and decrease in TR while low AMFR and high SOD decrease the possibility of abrasive embedment in the machined surface. Ahmed et al. [14] investigated the input parameters like hydraulic pressure, SOD, and TR for R_a of aluminum alloy 7075 during AWJ cutting. The RSM technique is used for modelling the surface smoothness and reported that WP and TR are the major considerable parameters. R_a can be minimized with

high jet pressure and low cutting speed. Prasad and Chaitanya [15] investigated the parameters for GFRP composite during hole drilling operation and found that various parameters which affect the process of delamination are thickness of material, feed rate, and orientation of fibre. Banon et al. [16] investigated carbon fibre reinforced thermoplastic polymer composite in three distinct regions: entry, centre, and outflow, and reported that surface quality is more affected in the entry zone, trailed by the outflow zone. Banon et al. [17] investigated the input parameters by using the response surface methodology (RSM) technique for carbon fibre reinforced thermoplastic matrix composite and revealed that surface quality is influenced by AMFR and WP. Kale et al. [18] suggested that the quality of cut depends on input parameters like WP, SOD, AMFR, abrasive type, TR, nozzle diameter, and for K_t ; AMFR and SOD are main substantial factors. Dahiya et al. [19] used Taguchi and GRA for optimization of process parameters for GFRP composites and revealed that R_a decreases with an increase in WP and decrease in TR. Impact of process parameters on R_a , K_t and metal removal rate (MRR) on armor steel has been investigated by Ram-mohan et al. [20] and a semi-empirical model was developed using Buckingham's pi theorem and regression equation. RSM based CCD approach is applied and impact of AWJM process parameters on K_t and R_a were investigated for Bismaleimide hybrid composite by Iyer et al. [21]. They revealed that for K_t minimization TR, WP and AMFR are the significant parameters and for R_a minimization TR is significant. A regression model was developed for prediction of jet penetration of non-through cut of carbon epoxy composite and found that adequacy of model was 96%. A mathematical model was also developed using these observations by Dhanawade et al. [22]. RSM-desirability technique was used for optimization of process parameters for kerf top width and kerf taper angle of Inconel600 during AWJM by Singh et al. [23]. RSM technique was applied to study the kerf properties of 6 mm thick mild steel with AWJM. ANOVA was used for analyzing the effect of various parameters for R_a and K_t . The desirability function was applied for multi-response optimization and the results were validated with confirmation tests [24]. Thakur et al. [25] reported that delamination at the jet entrance and exit of drilled hole decreases with decrease in SOD and TR for hybrid carbon/glass composite. RSM-based semi-analytical mathematical model has been developed for Titanium CFRP stacks and compared with a regression model to envisage hydro distortion defects by Pahuja and Ramulu [26]. Kumar et al. [27] developed a regression model using RSM for Kevlar49 epoxy composites for kerf taper during AWJM. MMR is investigated by Tripathi et al. [28] for GFRP during AWJM. A hybrid approach is used by Dhanawade et al. [22] to develop a mathematical model to predict the jet penetration in non through straight slit cuts on carbon fibre

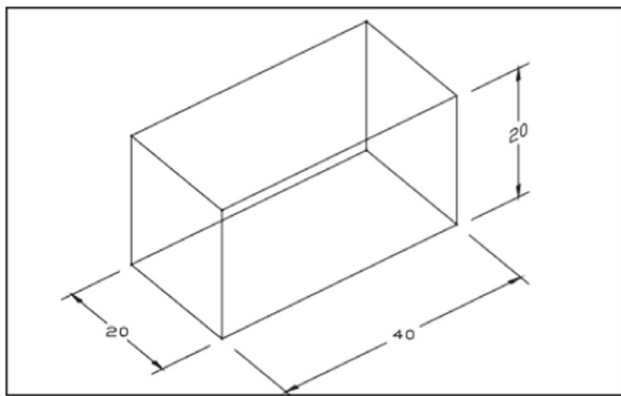


Fig. 3 Size of machined workpiece sample

reinforced polymer composite during AWJM. For optimization various techniques like RSM, metaphor-less algorithms, RMDTM, etc. are used by various researchers [29–32].

Some researchers have made efforts to study surface roughness and kerf geometry of machined composites during AWJM, but there have been less efforts reported to investigate defects like delamination, fibre pull-out, and abrasive embedment. To improve the kerf properties, researchers have initiated only one or two process parameters for optimization during AWJM of composites. But very less literature is available on multi-response optimization of process parameters related to AWJM of glass fibre reinforced polymer composite. The present work is focused on studying the effect of parameters (SOD, WP, TR, AMFR) on responses namely delamination, R_a and K_t for AWJM of GFRP composite. 2nd-order mathematical models are developed for responses, and the multi-response optimization is performed using desirability function for minimizing responses. Further, confirmation tests are performed for predictive models and optimising of process parameters during AWJM process. The subsequent section of this paper describes materials and methods.

2 Materials and methods

The experiments are performed on a flying arm CNC (Model-CNC DWJ2040-FB) abrasive water jet machine. The high-quality Garnet abrasives of size 80 mesh are selected for experimentation. The machine's nozzle assembly contains a 0.76 mm diameter nozzle and a sapphire jewel orifice having a diameter of 0.25 mm throughout the experiments, the impact angle is fixed at 90 degrees [33, 34]. GFRP composite of density 2.08 g/cm³, fibre diameter of 14 microns and volume fraction of glass fibre by weight 67% is used for experimentation. Dimensions (length-40 mm, width-20 mm and thickness-20 mm) of the machined specimen are as given in Fig. 3. Figure 4 displays the specimen cut by AWJM during experimentation.

In the present study four main parameters, specifically, WP, SOD, TR and AMFR with their levels are selected based on an exhaustive literature survey, pilot experiments and machining capability. Table 1 gives the selected process parameters for RSM based CCD approach, together with their respective alpha and centre point values. RSM is used to develop a 2nd order regression model for responses [35, 36]. Delamination in workpiece is measured using SEM and maximum crack length or maximum delamination length (Max. DLL) is taken for further analysis in this study. Surface roughness tester is used to measure the R_a of AWJ machined samples. A vision measurement system is used to measure the K_t . The K_t is determined by using the formula given below.

$$K_t = \tan^{-1}(W_t - W_b)/2t$$

where ' W_t '—kerf width at top, ' W_b '—kerf width at bottom and ' t '—workpiece material thickness

Defects like delamination of plies, fibre pullout and abrasive embedment are observed in SEM images of machined samples. ANOVA is performed to evaluate the significance and effects of various parameters on Max. DLL, R_a , and K_t . RSM's based CCD approach is used to develop the second-order regression models for Max. DLL, R_a and K_t . Further, RSM-Desirability approach is applied for multi-response optimization to minimize the responses.

3 Results and discussion

In this study, Design expert v13 software is used to analyze the experimental combinations recommended by the design matrix and experimental values of responses (Max. DLL, R_a and K_t) are given in Table 2. One of the most commonly used experimental designs for optimization is the response surface methodology (RSM). It is a useful method because it allows the evaluation of the efforts of multiple factors and their interactions with one or more response variables. The experiments are performed as per RSM design. RSM generates an array according to the CCD on four process parameters namely SOD, WP, TR and AMFR are considered to study their influence on response characteristics. The experimental design consists of a total of 30 experiments (an array with full factorial of two levels -16 experiments, an array of axial points—8 experiments and an array of centre points—6 experiments) Panneerselvam [37]. The relevance and impact of various parameters on Max. DLL, R_a and K_t are determined using ANOVA as displayed in Table 3.

ANOVA is performed for maximum delamination length as depicted in Table 3(a), WP, TR and AMFR are main significant process parameters and SOD is a less significant parameter. In quadratic terms, WP and AMFR have a

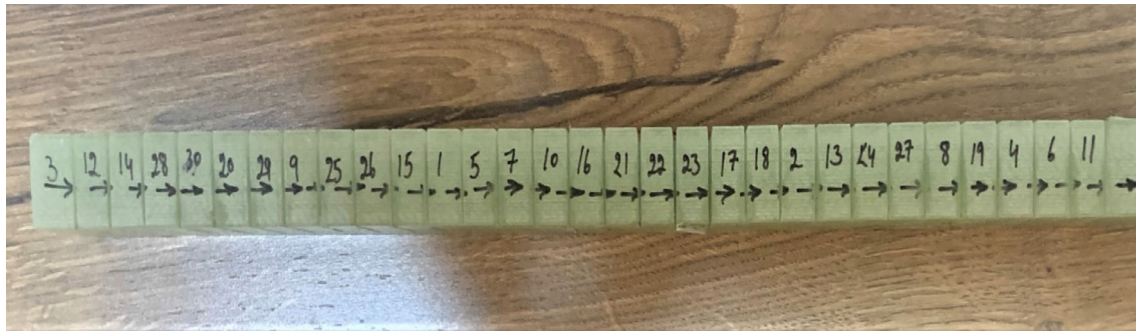


Fig. 4 Specimen cut by AWJM for experimentation

Table 1 Machining parameters with their levels

Parameters	Levels				
	− 2	− 1	0	1	2
SOD (A) in mm	1	2	3	4	5
WP (B) in MPa	120	140	160	180	200
TR (C) in mm/min	50	100	150	200	250
AMFR (D) in g/min	300	400	500	600	700

substantial impact and the remaining terms are less significant. Similarly, all parameters interactions with WP, TR and AMFR have a substantial impact. Here, the terms SOD, WP, TR and AMFR are denoted by A, B, C and D respectively. The F-value of model as highlighted in Table 3(a) is 29.27 and P-value less than 0.0001 shows that model is statistically substantial and has only a 0.01% chance due to noise. The F-value of 1.64 for lack of fit indicates that it is not significant in comparison with pure error.

To study the effects and identify the significance of parameters on R_a , ANOVA is performed. As given in ANOVA Table 3(b) for R_a ; WP, TR and AMFR are the main substantial terms trailed by SOD. From all these quadratic terms WP and AMFR are the main substantial parameters which have an impact on surface roughness and other parameters are insignificant. Similarly, parameter interactions between WP and TR have a substantial impact. The F-value 67.4 and P-value less than 0.0001 displays that model is substantial and in this model B, C, D, BC, B^2 , and D^2 are important terms. The lack of fit is not substantial with F-value of 2.38 which is related to the pure error.

ANOVA results given in Table 3(c) show that for kerf taper, SOD and WP are main substantial parameters trailed by TR and AMFR. In quadratic terms, AMFR has a major impact and interactions of SOD and WP, WP and TR, SOD and AMFR have significant results. For K_t as shown in ANOVA results Table 3(c) SOD and WP are main substantial parameters trailed by TR and AMFR. F-value of 65.94 and P-value less than 0.0001 shows that model is significant. In this model

terms A, B, C, D, AB, AC, AD, and D^2 are significant. F-value of 8.56 for lack of fit is related to pure error. K_t is mainly influenced by WP and SOD.

3.1 Influence of process parameters on responses

For Max. DLL, WP, TR and AMFR are major substantial process parameters and SOD is a less significant parameter. In quadratic terms, WP and AMFR have a substantial impact and the remaining terms are less significant. At high TR the amount of abrasive particles striking on workpiece material is reduced. As a result, overlapping of machining action is less. It increases the delamination of plies in machined samples. The cutting ability of the jet improves as AMFR increases as depicted in Fig. 5. The improved cutting capacity of the jet allows the material to cut smoothly through the laminates, resulting in minimal delamination.

The kinetic energy of a jet increases as pressure rises. The high kinetic energy jet cuts the laminates without deflection or wedging, resulting in less delamination. It indicates that delamination mainly occurs at bottom section of machined samples with high TR and low AMFR. The maximum delamination is experienced at bottom section of machined sample. SEM images in Fig. 6 show the Max. DLL (0.908 mm) in machined samples. All crack lengths that appeared on the machined sample surfaces caused by delamination are measured. The longest crack length, or maximum delamination, is taken into account for further analyses.

Other defects like fibre pullout and abrasive embedment are also observed in SEM images of machined samples

Table 2 Design matrix with process responses

Exp. no	A mm	B MPa	C mm/min	D g/min	R _a microns	K _t degree	Max. DLL mm
1	2	140	100	400	4.767	0.707	1.874
2	4	140	100	400	5.328	0.974	2.514
3	2	180	100	400	3.905	0.444	1.174
4	4	180	100	400	4.152	0.682	1.614
5	2	140	200	400	5.32	0.662	4.784
6	4	140	200	400	5.6	1.051	5.274
7	2	180	200	400	5.342	0.485	3.244
8	4	180	200	400	5.481	0.772	3.444
9	2	140	100	600	3.848	0.692	1.15
10	4	140	100	600	4.374	0.844	1.32
11	2	180	100	600	2.785	0.595	0.421
12	4	180	100	600	3.339	0.526	0.746
13	2	140	200	600	4.737	0.672	2.844
14	4	140	200	600	4.841	0.925	3.554
15	2	180	200	600	4.202	0.508	1.554
16	4	180	200	600	4.325	0.668	2.524
17	1	160	150	500	4.509	0.451	0.908
18	5	160	150	500	4.825	0.847	2.764
19	3	120	150	500	4.271	0.911	3.814
20	3	200	150	500	3.342	0.426	1.564
21	3	160	50	500	3.517	0.531	0.873
22	3	160	250	500	5.213	0.7	3.824
23	3	160	150	300	6.35	0.978	5.304
24	3	160	150	700	4.147	0.831	1.946
25	3	160	150	500	4.508	0.618	1.614
26	3	160	150	500	4.269	0.646	0.861
27	3	160	150	500	4.28	0.637	0.829
28	3	160	150	500	4.408	0.621	1.254
29	3	160	150	500	4.349	0.642	0.894
30	3	160	150	500	4.279	0.643	1.194

as shown in Fig. 7a and b. Fibre pull out is caused by highly targeted abrasive particles striking on workpiece during machining. It is particularly noticeable in machining with a low SOD and WP. The primary purpose of abrasives is to remove material by erosion. However, as AMFR increases, the number of abrasives striking on workpiece surface increases as well. Excessive abrasives penetrate the material's plies, causing abrasive embedment of abrasive particles, as illustrated in Fig. 7b. Embedment of abrasive particles in machined samples is mainly noticed at high AMFR and low SOD.

As given in Table 3(b) for R_a WP, TR and AMFR are main substantial terms trailed by SOD. From all these quadratic terms WP and AMFR are main substantial factors which have an impact on R_a and other parameters are insignificant.

Similarly, parameter interactions between WP and TR have a substantial impact. Effect of AMFR and TR on R_a is shown in Fig. 8. R_a is produced at lower TR and R_a increases with increase in TR. At high TR overlapping of abrasive particles are less, as a result, a rough surface is produced and similar results are reported [38, 39]. R_a decreases with an increase in AMFR as abrasive particles enhance the cutting ability of striking jet.

Wider kerf width is observed at top of machined sample and it decreases with increase in WP and decrease in TR of machined sample. Impact of WP and SOD on kerf taper is displayed in Fig. 9. Taper is produced towards the bottom region of machined samples as kinetic energy and pressure of jet are reduced. Similar results are reported by Shanmugam and Masood [40] in their study.

Table 3 ANOVA for (a) Max. DLL. (b) R_a (c) K_t

Source	SS	DOF	MS	F-value	P-value	
<i>(a) Max. DLL</i>						
Model	54.97	14	3.93	29.27	< 0.0001	Significant
A	2.4	1	2.4	17.87	0.0007	
B	7.16	1	7.16	53.37	< 0.0001	
C	20.77	1	20.77	154.83	< 0.0001	
D	11.4	1	11.4	84.98	< 0.0001	
A-B	0.0005	1	0.0005	0.0038	0.9518	
A-C	0.041	1	0.041	0.3057	0.5885	
A-D	0.0095	1	0.0095	0.0709	0.7937	
B-C	0.4802	1	0.4802	3.58	0.0779	
B-D	0.1109	1	0.1109	0.8267	0.3776	
CD	0.461	1	0.461	3.44	0.0835	
A ²	0.5665	1	0.5665	4.22	0.0577	
B ²	3.42	1	3.42	25.53	0.0001	
C ²	1.97	1	1.97	14.71	0.0016	
D ²	9.46	1	9.46	70.54	< 0.0001	
Residual	2.01	15	0.1341			
LF	1.54	10	0.1543	1.64	0.304	Insignificant
PE	0.4694	5	0.0939			
CT	56.98	29				
<i>(b) R_a</i>						
Model	16.25	14	1.16	67.42	< 0.0001	Significant
A	0.4176	1	0.4176	24.26	0.0002	
B	2.13	1	2.13	123.46	< 0.0001	
C	4.81	1	4.81	279.3	< 0.0001	
D	5.85	1	5.85	339.88	< 0.0001	
A-B	0.0104	1	0.0104	0.6044	0.449	
A-C	0.0964	1	0.0964	5.6	0.0318	
A-D	0.0004	1	0.0004	0.0232	0.8809	
B-C	0.558	1	0.558	32.41	< 0.0001	
B-D	0.0643	1	0.0643	3.73	0.0725	
C-D	0.0018	1	0.0018	0.1025	0.7533	
A ²	0.1734	1	0.1734	10.08	0.0063	
B ²	0.5044	1	0.5044	29.3	< 0.0001	
C ²	0.0004	1	0.0004	0.0258	0.8746	
D ²	1.39	1	1.39	80.59	< 0.0001	
Residual	0.2582	15	0.0172			
LF	0.2134	10	0.0213	2.38	0.1753	Insignificant
PE	0.0448	5	0.009			
CT	16.51	29				
<i>(c) K_t</i>						
Model	0.8048	14	0.0575	65.94	< 0.0001	Significant
A	0.254	1	0.254	291.33	< 0.0001	

Table 3 (continued)

Source	SS	DOF	MS	F-value	P-value	
B	0.3306	1	0.3306	379.25	< 0.0001	
C	0.0159	1	0.0159	18.19	0.0007	
D	0.0171	1	0.0171	19.64	0.0005	
AB	0.0124	1	0.0124	14.2	0.0019	
AC	0.0157	1	0.0157	17.99	0.0007	
AD	0.0293	1	0.0293	33.64	< 0.0001	
BC	0.0005	1	0.0005	0.62	0.4433	
BD	0.0019	1	0.0019	2.2	0.1591	
CD	0.0001	1	0.0001	0.1584	0.6963	
A ²	0.0001	1	0.0001	0.1435	0.7102	
B ²	0.0013	1	0.0013	1.55	0.2328	
C ²	0.0011	1	0.0011	1.22	0.2858	
D ²	0.1195	1	0.1195	137.08	< 0.0001	
Residual	0.0131	15	0.0009			
Lack of fit	0.0124	10	0.0012	8.56	0.0143	Not significant
Pure error	0.0007	5	0.0001			
Cor. total	0.8179	29				

3.2 Regression models

RSM-based CCD approach is applied for building a 2nd order mathematical model to predict the responses without a complete three-level full factorial design. Best-fitted empirical model, which establishes a correlation between responses with the given process parameters (WP, TR, SOD, AMFR) is developed using RSM. Regression models are fitted to surfaces produced by independent variables in this approach. As a result, 2nd order quadratic models are developed based on experimental analysis to depict the response surfaces that fit the data as stated in Eqs. 1, 2 and 3 for Max. DLL, R_a and K_t respectively. The regression equation in actual terms for the Max. DLL is given below as Eq. 1.

$$\begin{aligned}
 \text{Max. DLL} = & 114.746 + -0.73 \times \text{SOD} + -1.17325 \\
 & \times \text{WP} + 0.0557975 \times \text{TR} \\
 & + -0.0745838 \times \text{AMFR} + -0.0005625 \\
 & \times \text{SOD} \times \text{WP} + 0.0010125 \times \text{SOD TR} \\
 & + 0.00024375 \times \text{SOD AMFR} + \\
 & - 0.0003465 \times \text{WP TR} + 8.325e - 05 \times \text{WP AMFR} \\
 & + -3.395e - 05 \times \text{TR AMFR} \\
 & + 0.143708 \times \text{SOD}^2 + 0.00353333 \\
 & \times \text{WP}^2 + 0.000107283 \times \text{TR}^2 \\
 & + 5.87333e - 05 \times \text{AMFR}^2
 \end{aligned} \quad (1)$$

The predicted R-squared value (0.8322) is near to adjusted R-squared value (0.9317). Figure 10 shows the graph

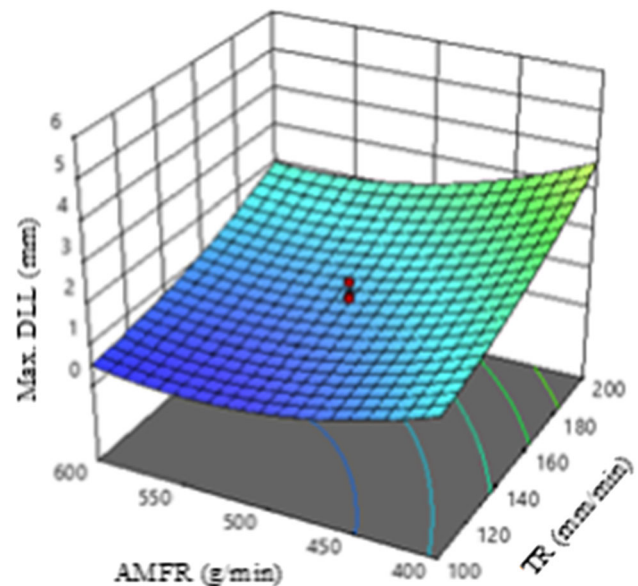


Fig. 5 Impact of TR and AMFR on Max.DLL

between predicted vs actual values for Max. DLL. All experimental values are close to the best fit line with a predicted R² value of 0.8322 which shows that model is significant.

The regression equation for the R_a in actual terms is given below as Eq. 2.

$$\begin{aligned}
 R_a = & 6.02423 + 0.0666667 \times \text{SOD} + 0.0852604 \times \text{WP} \\
 & + -0.0178033 \times \text{TR} + -0.0228221 \times \text{AMFR} \\
 & + -0.001275 \times \text{SOD} \times \text{WP} +
 \end{aligned}$$

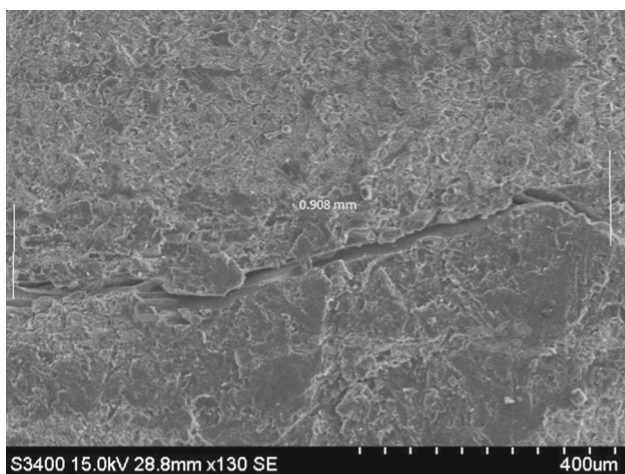


Fig. 6 SEM images for Max. DLL in machined samples

$$\begin{aligned}
 & - 0.0015525 \times \text{SOD} \times \text{TR} + 5e - 05 \\
 & \times \text{SOD} \times \text{AMFR} + 0.00018675 \times \text{WP} \\
 & \times \text{TR} + \\
 & - 3.16875e - 05 \times \text{WP} \times \text{AMFR} \\
 & + 2.1e - 06 \times \text{TR} \times \text{AMFR} + 0.0795208 \\
 & \times \text{SOD}^2 + \\
 & - 0.00033901 \times \text{WP}^2 + 1.60833e \\
 & - 06 \times \text{TR}^2 + 2.24896e - 05 \times \text{AMFR}^2 \quad (2)
 \end{aligned}$$

The predicted R² value (0.9844) is near to adjusted R² value (0.9698). Figure 11 shows the graph between predicted vs actual values for R_a. All experimental values are close to the best fit line with a predicted R² value of 0.9844 which shows that model is significant.

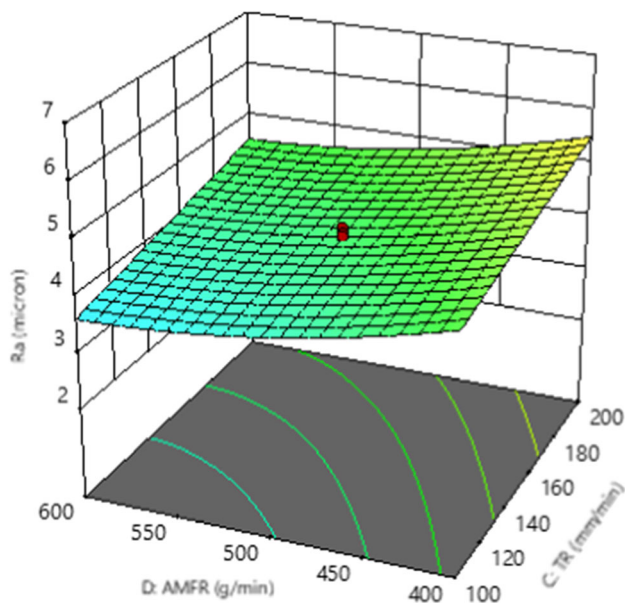


Fig. 8 Impact of AMFR and TR on R_a

The regression equation for the K_t in actual terms is given below as Eq. 3.

$$\begin{aligned}
 K_t = & 2.88834 + 0.432687 \times \text{SOD} + -0.0109115 \times \text{WP} \\
 & + -0.00125208 \times \text{TR} + -0.00637063 \times \text{AMFR} \\
 & + -0.00139062 \times \text{SOD WP} \\
 & + 0.00062625 \times \text{SOD TR} + -0.000428125 \\
 & \times \text{SOD AMFR} + 5.8125e - 06 \times \text{WP TR} + 5.46875e \\
 & - 06 \times \text{WP AMFR} + \\
 & - 5.875e - 07 \times \text{TR AMFR} + 0.00213542 \times \text{SOD}^2 \\
 & + 1.7526e - 05 \times \text{WP}^2 + -2.49583e
 \end{aligned}$$

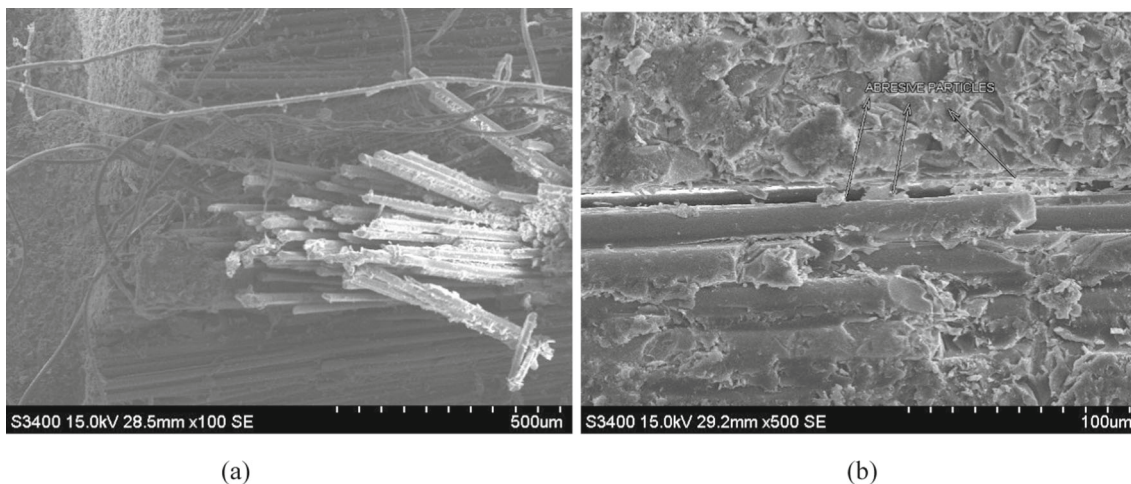


Fig. 7 SEM images a Fibre pull out b abrasive embedment

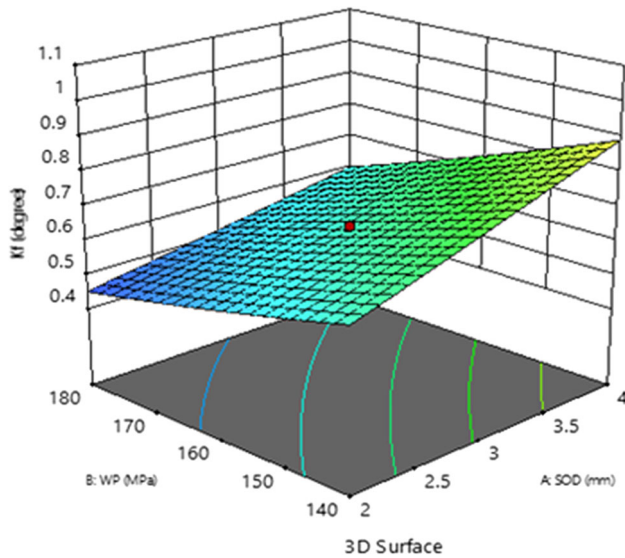


Fig. 9 Impact of WP and SOD on K_t

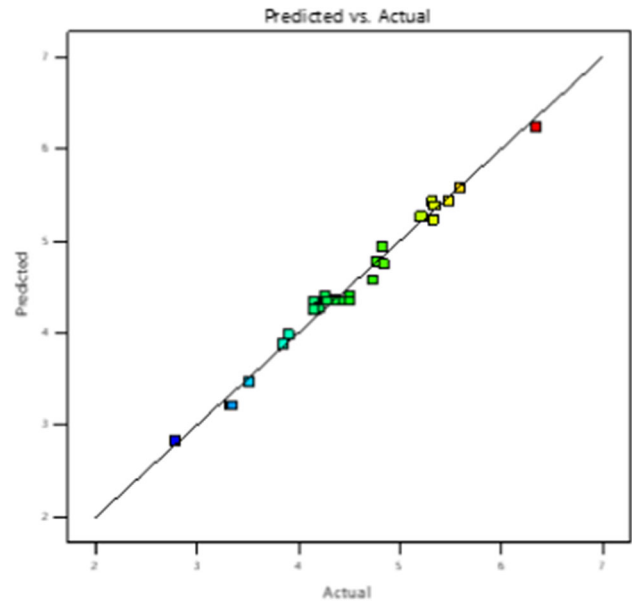


Fig. 11 Predicted versus Actual for R_a

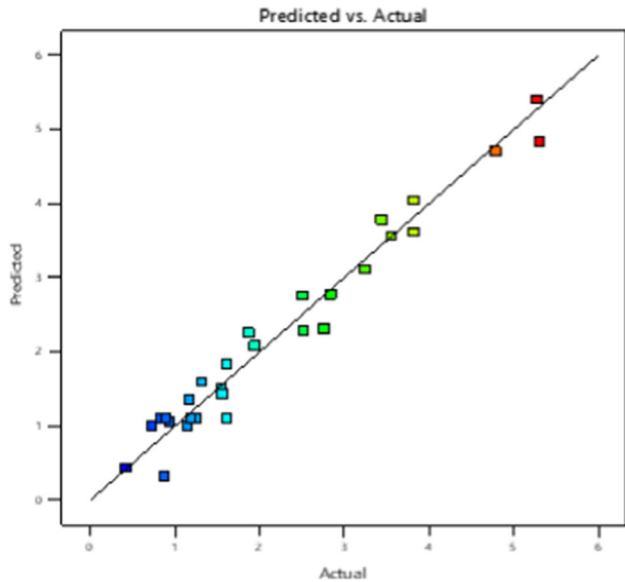


Fig. 10 Predicted versus Actual for Max. DLL

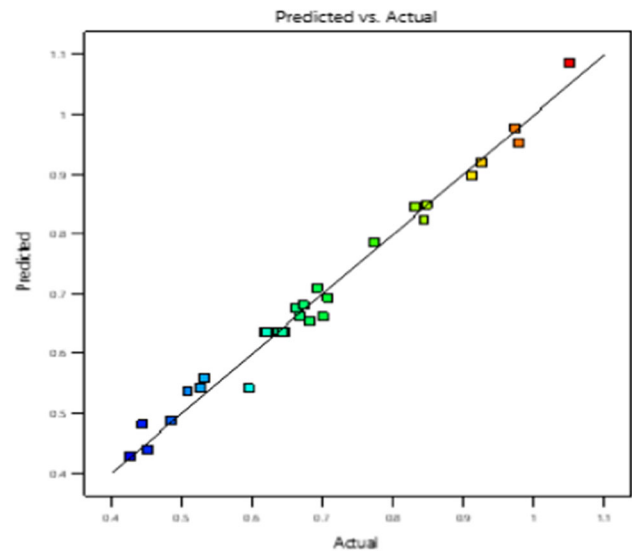


Fig. 12 Predicted versus Actual Values for K_t

$$- 06 \times TR^2 + 6.60104e - 06 \times AMFR^2 \quad (3)$$

The predicted R-squared (0.9840) is reasonably close to the adjusted R-squared (0.9691). Figure 12 shows the graph between predicted vs actual values for K_t . All experimental values are close to the best fit line with a predicted R^2 value of 0.984 which shows that model is significant.

3.3 Optimization of process parameters

For optimization, the desirability function is used. To minimize the delamination length and enhance the kerf geometry

multi-response optimization of input parameters is performed by selecting the target for process parameters (in range) and responses (minimize/ target). The desirability function is used to convert the multi-response to single-response characteristics. All responses are transformed into a desirability function in this method. This approach is a popular way of assigning a “score” to a group of responses and selecting factor settings to maximize that score. This approach is extensively used in the industry for optimizing various response characteristics. Desirability technique is used for determining the optimum solution [41]. It is an

Table 4 Multi-optimization of parameters

Parameters/Response	Units	Target	Lower value	Upper value	Optimized values
SOD	mm	In-range	1	5	2
WP	MPa	In-range	120	200	180
TR	mm/min	In-range	50	250	100
AMFR	g/min	In-range	300	700	534
Max. DLL	mm	Target(0.421)	0.421	5.304	0.421
R _a	microns	Minimize	2.785	6.35	3.013
K _t	degree	Minimize	0.426	1.051	0.462

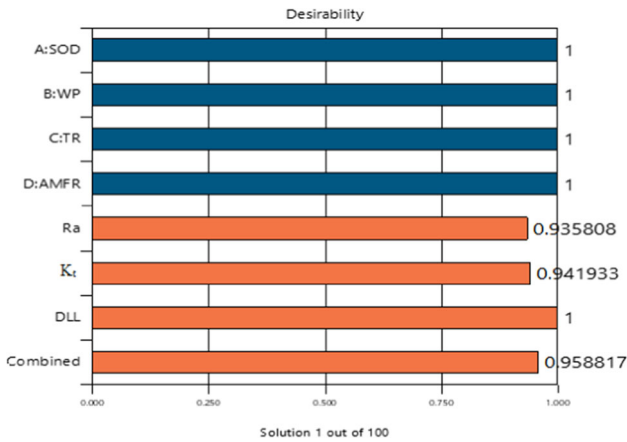


Fig. 13 Bar graph for desirability

objective function with a value of one at the goal and zero outside of the limits. It's predicated on the premise that a product or process with many quality attributes, one of which is outside of some "desired" boundaries, is utterly undesirable.

To minimize the Max. DLL, K_t and R_a multi-response optimization technique is applied. For multi-response optimization, RSM-Desirability approach is used [42–46]. For all responses, the importance and weights are the same. Table 4 shows the best solution for minimizing Max. DLL, R_a, and K_t using Design Expert v13 software. The optimized values of R_a, K_t and Max. DLL are 3.013, 0.462 and 0.421 respectively at optimized set of parameters. Similar results are reported by Dhanawade and Kumar [39] in their study. The bar graph in Fig. 13 depicts the desirability score of all parameters and responses. Desirability of all response factors has a value of 1. R_a, K_t, and delamination have desirable values of 0.936, 0.942 and 1 respectively. These values of desirability are acceptable. All process parameters and responses have a combined desirability rating of 0.959, which is reasonably good and acceptable. Figure 14 shows the combined desirability at optimum levels. Optimum parameters are extremely useful for examining individual reaction behaviour in proximity of the optimal condition.

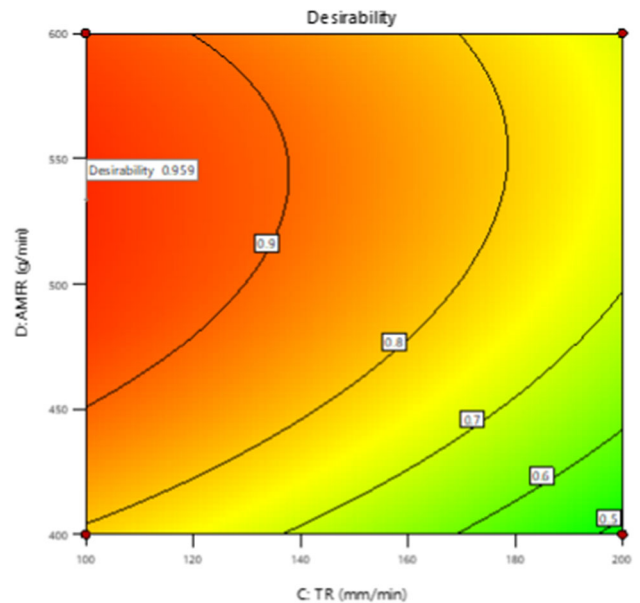


Fig. 14 Combined desirability value at optimum levels

3.4 Confirmation tests

Confirmation tests are performed for predictive models and at the optimum level of parameters. Within the scope, several random combinations of parameters are chosen. For 2nd order quadratic models, confirmation tests are performed for R_a, K_t and Max. DLL to verify the adequacy of the model. Actual and predicted values are compared to calculate the errors. For confirmation tests, experiment run numbers 8, 13, 23 and 25 are selected randomly. The result of the confirmation test for responses is summarized in Table 5. The percentage error between experimental and predicted values for responses is small. The results of confirmation trials are found to be in good accord with the predicted response values. The percentage error between experimental and predicted values for R_a is less than 1.977, for K_t is less than 3.156 and for Max. DLL is less than 7.252 which is small and acceptable.

Figure 15 shows the bar graph between the experimental and their corresponding predicted values for R_a, K_t and Max.

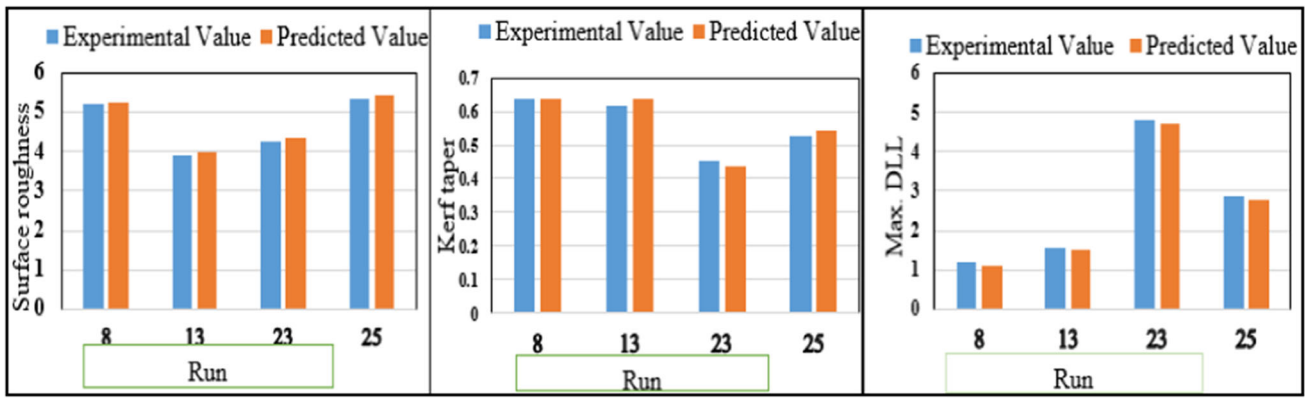


Fig. 15 Bar graph between experimental and predicted values for R_a , K_t and Max. DLL

Table 5 Confirmation test for predictive models

Run	Surface roughness (R_a)				Kerf taper (K_t)				Max. DLL			
	Experimental value	Predicted value	Residual	Error (%)	Experimental value	Predicted value	Residual	Error (%)	Experimental value	Predicted value	Residual	Error (%)
8	5.210	5.260	-0.047	-0.904	0.637	0.635	0.003	0.392	1.190	1.110	0.086	7.252
13	3.900	3.980	-0.073	-1.879	0.618	0.635	-0.017	-2.670	1.550	1.510	0.044	2.839
23	4.280	4.350	-0.069	-1.607	0.451	0.437	0.014	3.038	4.780	4.700	0.080	1.669
25	5.320	5.430	-0.105	-1.977	0.526	0.543	-0.017	-3.156	2.840	2.770	0.073	2.567

Table 6 Confirmation test for optimized values

Exp	Surface roughness			Kerf taper			Delamination		
	Optimized value	Experimental value	Error (%)	Optimized value	Experimental value	Error (%)	Optimized value	Experimental value	Error (%)
1	3.013	3.109	3.088	0.462	0.498	7.229	0.421	0.439	4.100
2		2.907	-3.646		0.459	-0.654		0.432	2.546
3		3.216	6.312		0.477	3.145		0.440	4.318
4		3.089	2.460		0.469	1.493		0.426	1.174

DLL. It was found very small variation between experimental and predicted results. Bar graphs show that experimental results closely match the predicted results.

During the machining of GFRP with AWJM, four experiments are conducted for the confirmation tests at optimum levels of parameters. Table 6 shows the results of confirmation tests at an optimum level of process parameters ($SOD = 2$ mm, $WP = 180$ MPa, $TR = 100$ mm/minute and $AMFR = 534$ g/min). Confirmation tests are performed to validate the experimental values and optimized level of parameters which show less than 6.312% of error for R_a , 7.229% of error for K_t and 4.318% of error for Max. DLL.

Bar graphs in Fig. 16 show that the experimental results of response (R_a , K_t and Max. DLL) are very near to the optimized values. It is been observed that optimized values

of parameters give the optimum solution for minimizing the R_a , K_t and Max. DLL.

4 Conclusions

In this paper, parametric investigation on maximum delamination length, surface roughness and kerf taper for AWJM of GFRP composite has been described using RSM based CCD approach and RSM based Desirability approach is used for multi-response optimization. Based on the experimental modelling and optimization results, the following conclusions are summarized:

- i. From the response surface plot it has been observed that the abrasive mass flow rate and traverse rate are

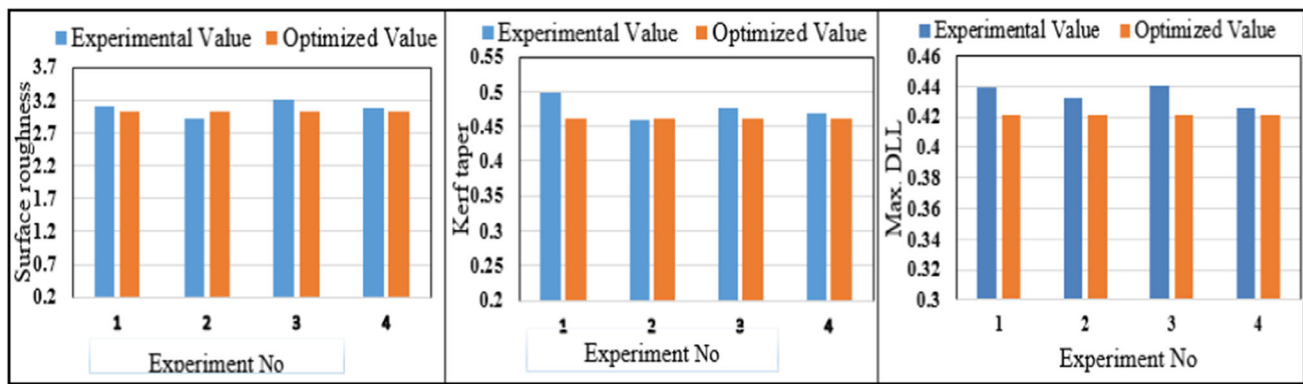


Fig. 16 Bar graph between experimental and optimized value for R_a , K_t and Max. DLL

the most substantial process parameters followed by water pressure in influencing delamination. Delamination decreases with decrease in traverse rate and standoff distance and increase in water pressure and abrasive mass flow rate. It is also found that the surface roughness decreases with increase in water pressure and decrease in traverse rate; while kerf taper decreases with increase in water pressure and decrease in standoff distance.

- ii. The developed response surface models for Max DLL, R_a and K_t using CCD matrix have been found adequate at 99% confidence level. It has also been analyzed from the results of regression coefficients that the linear effects of process parameters are significant for all the models. The results of confirmation tests are found to be in good accord with the predicted response values
- iii. During the experiments it has been seen that fibre pull-out was obtained at low water pressure as well as higher stand-off distance and Embedment of abrasive particles were also noticed at high abrasive mass flow rate as well as low stand-off distance
- iv. Further, Multi-response optimization of process parameters has also been performed using the desirability approach to minimize these response characteristics. At optimum set of process parameters, the optimized values of Max. DLL, R_a and K_t have been found 3.013 μm , 0.462° and 0.42 mm respectively. Confirmation tests are also performed to validate the experimental results.

The findings of the present study are certainly useful for effective process planning of AWJM of GFRP composite to produce defect-free parts. In future, efforts may be extended in the following directions:

- i. Experimental investigation of AWJM of hybrid composites, as these materials have wide applications in aerospace, structural and transportation sectors.
- ii. Effects of tool wear and nozzle wear can be examined on influencing machining performance

References

- Campbell, F.C.: Introduction to Composite Materials, Structural Composite, Materials, ASM International, USA (2010)
- Kovacevic, R., Hashish, M., Mohan, R., Ramulu, M., Kim, T.J., Geskin, E.S.: State of the art of research and development in abrasive water jet machining. *J. Manuf. Sci. Eng.* **119**, 776–785 (1997). <https://doi.org/10.1115/1.2836824>
- Jain, V.K.: Advanced Machining Processes. Allied publishers private limited, New Delhi (2005)
- Momber, A.W., Kovacevic, R.: Principles of abrasive water jet machining. Springer Science & business media, London (1998)
- Dahiya, A.K., Bhuyan, B.K., Kumar, S.: Perspective study of abrasive water jet machining of composites—a review. *J. Mech. Sci. Technol.* **36**, 213–224 (2022). <https://doi.org/10.1007/s12206-021-1220-x>
- Dahiya, A.K., Bhuyan, B.K., Kumar, S.: A Review on Machining Potential of Composite Materials During Abrasive Water Jet Machining. *Lect. Notes Mech. Eng.* 1301–1315 (2022) https://doi.org/10.1007/978-981-16-2794-1_111
- Kuttan, A.A., Rajesh, R., DevAnand, M.: Abrasive water jet machining techniques and parameters: a state of the art, open issue challenges and research directions. *J. Braz. Soc. Mech. Sci. Eng.* **43**(220), 1–14 (2021). <https://doi.org/10.1007/s40430-021-02898-6>
- Lemma, E., Chen, L., Siores, E., Wang, J.: Study of cutting fiber-reinforced composites by using abrasive water-jet with cutting head oscillation. *Compos. Struct.* **57**, 297–303 (2002). [https://doi.org/10.1016/S0263-8223\(02\)00097-1](https://doi.org/10.1016/S0263-8223(02)00097-1)
- Azmir, M.A., Ahsan, A.K.: Investigation on glass/epoxy composite surfaces machined by abrasive water jet machining. *J. Mater. Process. Technol.* **198**, 122–128 (2007). <https://doi.org/10.1016/j.jmatprotec.2007.07.014>
- Shanmugam, D.K., Nguyen, T., Wang, J.: A study of delamination on graphite/epoxy composites in abrasive water jet machining. *Compos. Part A* **39**, 923–929 (2008)
- Izzet, K., Gokhan, A., Kerim, A.: An investigation on the kerf width in abrasive waterjet cutting of granitic rocks. *Arab. J. Geosci.* **7**, 2923–2932 (2014). <https://doi.org/10.1007/s12517-013-0984-4>
- Alberdi, A., Artaza, T., Suarez, A., Rivero, A., Girof, F.: An experimental study on abrasive waterjet cutting of CFRP/Ti6Al4V stacks for drilling operations. *Int. J. Adv. Manuf. Technol.* (2016). <https://doi.org/10.1007/s00170-015-8192-x>
- Dhanawade, A., Kumar, S., Kalmekar, R.V.: Abrasive Water Jet Machining of Carbon Epoxy Composite. *Def. Sci. J.* **66**(5), 522–528 (2016)

14. Ahmed, T.M., Mesalamy, A.S., Youssef, A., Midany, T.T.: Improving surface roughness of abrasive waterjet cutting process by using statistical modelling. *CIRP J. Manuf. Sci. Technol.* **22**, 30–36 (2018). <https://doi.org/10.1016/j.cirpj.2018.03.004>
15. Prasad, S.K., Chaitanya, G.: Analysis of delamination in drilling of GFRP composites using Taguchi Technique. *Mater. Today Proc.* **18**(7), 3252–3261 (2019)
16. Banon, F., Sambruno, A., Ruiz-Gracia, R., Salgueroet, J., Mayuet, P.F.: Study of the influence of cutting parameters on surface quality in AWJM machining of thermoplastic matrix composites. *Proc. Manuf.* **41**, 233–242 (2019). <https://doi.org/10.1016/j.promfg.2019.07.051>
17. Banon, F., Sambruno, A., Batista, M., Simonet, B., Salgueroet, J.: Study of the surface quality of carbon fiber–reinforced thermoplastic matrix composite (CFRTP) machined by abrasive water jet (AWJM). *Int. J. Adv. Manuf. Technol.* **107**, 3299–3313 (2020)
18. Kale, A., Singh, S.K., Sateesh, N., Subbiah, R.: A review on abrasive water jet machining process and its process parameters. *Mater. Today: Proc.* **26**(2), 1032–1036 (2020). <https://doi.org/10.1016/j.matpr.2020.01.309>
19. Dahiya, A.K., Bhuyar, B.K., Kumar, S.: Optimization of process parameters for surface roughness of GFRP with AWJ machining using Taguchi and GRA methods. *Int. J. Mod. Manuf. Technol.* **13**(2), 2021 (2021)
20. Rammohan, S., Kumaran, S.T., Uthayakumar, M., Korniejenko, K., Nykiel, M., Velayutham, A.: Prediction of abrasive waterjet machining parameters of military-grade armor steel by semi-empirical and regression models. *Materials*. **15**, 4368 (2022). <https://doi.org/10.3390/ma15124368>
21. Iyer, N.P., Arunkumar, N.: Investigation of abrasive water jet machining parameters of Bismaleimide composites. *Mater. Manuf. Process.* (2022). <https://doi.org/10.1080/10426914.2022.2032145>
22. Dhanawade, A., Wazarkar, S., Kumar, S.: Erosion model for abrasive water jet machining of composite materials. *J. Braz. Soc. Mech. Sci. Eng.* **44**, 268 (2022). <https://doi.org/10.1007/s40430-022-03565-0>
23. Singh, D., Shukla, R.S.: Investigation of kerf characteristics in abrasive water jet machining of inconel 600 using response surface methodology. *Def. Sci. J.* **70**(3), 312–322 (2020)
24. Dumbhare, P.A., Dubey, S., Deshpande, Y.V., Andhare, A.B., Barve, P.S.: Modelling and multi-objective optimization of surface roughness and kerf taper angle in abrasive water jet machining of steel. *J. Braz. Soc. Mech. Sci. Eng.* **40**, 259 (2018). <https://doi.org/10.1007/s40430-018-1186-5>
25. Thakur, R.K., Singh, K.K., Ramkumar, J.: Delamination analysis and hole quality of hybrid FRP composite using abrasive water jet machining. *Mater. Today: Proc.* **33**(8), 5653–5658 (2020)
26. Pahuja, R., Ramulu, M.: Abrasive water jet machining of Titanium (Ti6Al4V)–CFRP stacks—a semi analytical modeling approach in the prediction of kerf geometry. *J. Manuf. Process.* **39**, 327–337 (2019). <https://doi.org/10.1016/j.jmapro.2019.01.041>
27. Kumar, P., Salunkhe, S., Kant, R.: Experimental investigation of kerf characteristics of kevlar49 epoxy composite machined by abrasive water jet. *Int. J. Mod. Manuf. Technol.* **11**(2), 13–18 (2019)
28. Tripathi, D.R., Vachhani, K.H., Kumari, S., et al.: Experimental investigation on material removal rate during abrasive water jet machining of GFRP composites. *Mater. Today Proc.* **26**(2), 1389–1392 (2020). <https://doi.org/10.1016/j.matpr.2020.02.280>
29. Tripathi, D.R., Vachhani, K.H., Bandhu, D., et al.: Experimental investigation and optimization of abrasive waterjet machining parameters for GFRP composites using metaphor-less algorithms. *Mater. Manuf. Process.* **36**(7), 803–813 (2021)
30. Bandhu, D., Abhishek, K.: Assessment of weld bead geometry in modified shortcircuiting gas metal arc welding process for low alloy steel. *Mater. Manuf. Process.* **36**(12), 1384–1402 (2021)
31. Bandhu, D., Kumari, S., Prajapati, V.K., et al.: Experimental investigation and optimization of RMDTM welding parameters for ASTM A387 grade 11 steel. *Mater. Manuf. Process.* **36**(13), 1524–1534 (2021)
32. Dinbandhu, Abhishek, K.: Parametric Optimization and Evaluation of RMD™ Welding Performance for ASTM A387 Grade 11 Steel Plates Using TOPSIS-Taguchi Approach. In: Patnaik, A., Kozeschnik, E., Kukshal, V. (eds) *Advances in Materials Processing and Manufacturing Applications*. iCADMA 2020. Lecture Notes in Mechanical Engineering. (2021) Springer, Singapore. https://doi.org/10.1007/978-981-16-0909-1_22
33. Natarajan, Y., Murugesan, P.K., Mohan, M., Khan, S.A.L.A.: Abrasive water jet machining process: a state of art of review. *J. Manuf. Process.* **49**, 271–322 (2020). <https://doi.org/10.1016/j.jmapro.2019.11.030>
34. Llanto, J.M., Tolouei-Rad, M., Vafadar, A., Aamir, M.: Recent progress trend on abrasive waterjet cutting of metallic materials: a review. *Appl. Sci.* **11**, 3344 (2021). <https://doi.org/10.3390/app11083344>
35. Montgomery, D.C.: *Design and analysis of experiments*. Wiley, New York (1997)
36. Basanta, B.K., Yadava, V.: Experimental modelling and multi-response optimization of travelling wire electrochemical spark machining of Pyrex glass. *Proc. Inst. Mech. Eng. B J. Eng. Manuf.* **228**(8), 902–916 (2014). <https://doi.org/10.1177/0954405413514745>
37. Panneerselvam, R.: *Design and Analysis of Experiments*. PHI learning, Delhi (2012)
38. Azmir, M.A., Ahsan, A.K.: Study of abrasive water jet machining process on glass/ epoxy composite laminate. *J. Mater. Process. Technol.* **209**(20), 6169–6173 (2009). <https://doi.org/10.1016/j.jmatprotec.2009.08.011>
39. Dhanawade, A., Kumar, S.: Abrasive water jet machining of carbon epoxy composite: cutting performance, predictive models and optimization. *Indian Journal of Engineering & Material Sciences.* **26**, 265–275 (2019)
40. Shanmugam, D.K., Masood, S.: An investigation on kerf characteristics in abrasive waterjet cutting of layered composites. *J. Mater. Process. Technol.* **209**, 3887 (2009)
41. Dhanawade, A., Kumar, P., Kumar, S.: Experimental study on abrasive water jet machining of carbon epoxy composite. *Adv. Mater. Process. Technol.* **6**(1), 40–53 (2020). <https://doi.org/10.1080/2374068X.2019.1703338>
42. Fuse, K., Chaudhari, R., Jayvora, J., Patel, V.K., de Lacalle, L.N.L.: Multi-Response optimization of abrasive waterjet machining of Ti6Al4V using integrated approach of utilized heat transfer search algorithm and RSM. *Materials* **14**, 7746 (2021)
43. Kolli, M., RamPrasad, A.V.S., Naresh, D.S.: Multi-objective optimization of AAJM process parameters for cutting of B4C/Gr particles reinforced Al 7075 composites using RSM-TOPSIS approach. *SN Appl. Sci.* **3**, 711 (2021). <https://doi.org/10.1007/s42452-021-04699-x>
44. Gnanavelbabu, A., Arunachalam, V., SunuSurendran, K.T., Saravanan, P.: Optimization of abrasive water jet machining parameters on AA6061/B4C/hBN hybrid composites using grey-RSM. *IOP Conf. Ser. Mater. Sci. Eng.* **764**, 012011 (2020). <https://doi.org/10.1088/1757-899X/764/1/012011>
45. Thamizhvalavan, P., Yuvaraj, N., Arivazhagan, S.: Abrasive water jet machining of Al6063/B4C/ZrSiO4 hybrid composites: a study

- of machinability and surface characterization analysis. SILICON **14**, 1093–1121 (2022). <https://doi.org/10.1007/s12633-020-00888-2>
46. Dahiya, A.K., Bhuyan, B.K., Acharya, V., Kumar, S.: Optimization of process parameters for machining defects of glass fibre reinforced polymer composite machined by AWJM. Mater. Today Proc. (2022). <https://doi.org/10.1016/j.matpr.2022.12.138>

Publisher's Note Springer Nature remains neutral with regard to jurisdictional claims in published maps and institutional affiliations.

Springer Nature or its licensor (e.g. a society or other partner) holds exclusive rights to this article under a publishing agreement with the author(s) or other rightsholder(s); author self-archiving of the accepted manuscript version of this article is solely governed by the terms of such publishing agreement and applicable law.